PNAS
www.pnas.org

Supplementary Information for

Coordination of Cell Migration Mediated by Site-Dependent Cell-Cell Contact

David Li[1] and Yu-li Wang[1]

[1]Department of Biomedical Engineering
Carnegie Mellon University
5000 Forbes Avenue
Pittsburgh, PA 15213
USA

Corresponding Author:
Yu-li Wang
Email: yuliwang@andrew.cmu.edu

This PDF file includes:

Supplementary text
Figs. S1 to S7
Tables S1 to S2
Captions for movies S1 to S13
References for SI reference citations

Other supplementary materials for this manuscript include the following:

Movies S1 to S13

www.pnas.org/cgi/doi/10.1073/pnas.1807543115

Supplementary Information Text

SI Materials and Methods

Cell culture. NRK-52E rat kidney epithelial cells, NIH 3T3 mouse fibroblasts, and MDCK mouse kidney epithelial cells were obtained from American Type Culture Association (Manassas, VA) and maintained in Dulbecco's modified Eagle's medium (Life Technologies, Carlsbad, CA) supplemented with 10% fetal bovine serum (for MDCK and NRK-52E cells, Thermo Scientific, Waltham, MA) or 10% donor bovine serum (for NIH 3T3 cells), 50 µg/mL streptomycin, 50 U/mL penicillin, and 2 mM L-glutamine (Life Technologies, Carlsbad, CA) (1-2). All cells were maintained in an incubator with 5% CO2 at 37ºC. Prior to seeding, cells were treated with 30 µM mitomycin (Calbiochem, San Diego, CA) for 2 hrs to avoid complications due to cell division (3). Mitomycin treatment did not affect migration speed, persistence, or symmetry breaking. Dishevelled activity was inhibited by overnight treatment with either 50 µM NSC 668036 (Sigma-Aldrich, St. Louis, MO), prepared from a 5 mM stock solution in PBS (4), or 10 µM 3289-8625 (Sigma-Aldrich, St. Louis, MO), prepared from a 5mM stock solution in DMSO (5). Myosin II-mediated contractility was inhibited by incubating cells in 50 µM (-)-blebbistatin (Sigma-Aldrich, St. Louis, MO), prepared from a 100 mM stock solution in DMSO by diluting slowly into media under vigorous stirring followed by filtration through a 0.22 µm filter.

Preparation of micropatterned polyacrylamide substrates. Micropatterned polyacrylamide (PA) substrates were prepared as described previously (6). A 0.1% (w/v) solution of 50 Bloom gelatin was first activated with 3.5 mg/mL sodium m-periodate (Sigma-Aldrich, St. Louis, MO) at room temperature for 30 min. Polydimethylsiloxane stamps were fabricated with micropatterns of strips 30 µm in width, via soft lithography. Intersections between crossing strips were spaced at least 1 mm apart. The stamps were incubated in a solution of activated gelatin and excess solution was blown off using nitrogen gas. The stamp was then pressed on a clean glass coverslip to transfer the patterned gelatin. Acrylamide solution was prepared to contain a final concentration of 8% acrylamide, 0.2% bis-acrylamide, and a 1:1000 dilution of 0.2 µm fluorescent polystyrene beads (Molecular Probes, Carlsbad, CA) (7). This solution was degassed in a vacuum chamber for at least 30 minutes before adding the initiators ammonium persulfate (Sigma Aldrich, St. Louis, MO) and N,N,N',N' tetramethylethylenediamine (Bio-Rad, Hercules, CA). A volume of 30 µL of this solution was placed on a large glass coverslip previously treated with 0.3% (v/v) Bind-Silane (GE Healthcare, Waukesha, WI) in 95% ethanol. The micropatterned coverslip was then placed on top of the drop as acrylamide polymerized. After polymerization for 20 min, the top coverslip was removed with a pair of fine tweezers and the bottom coverslip was mounted into a custom chamber dish. Before use, the substrate was sterilized under 260 nm ultraviolet light for 30 min and rinsed briefly with cell culture media. NRK-52E cells were seeded onto the substrate and incubated for 12-18 hrs before experiments to allow attachment, unless otherwise noted. Collectives of 5-6-cells were obtained by plating cells on the substrates at a density of ~2500 cells/mL followed by ~12 hrs of incubation.

Assessment of the responses of cell migration to cell-cell contact. Responses of cell migration to cell-cell contact were characterized through interactions between cells stalled at X or T intersections and cells migrating nearby. Phase contrast images of cells were taken every 10 min over at least 12 hrs with a Nikon Eclipse Ti microscope equipped with a 10x PlanFluor dry phase contrast objective lens and on-stage culture chamber. Tracking at multiple sites was facilitated using a motorized stage and the Perfect Focus mechanism for maintaining the focus at each location.

The effect of cell-cell contact on symmetry breaking was determined in a double seeding experiment, where cells were seeded in two rounds, 2 hrs apart, on PA substrates micropatterned

with 30 μm adhesive strips. A density of ~ 600 cells/mL was used for both rounds of seeding. Observations started after six hours past the first seeding time.
Two cells were considered interacting if their discernable membranes came within <20 μm for at least 10 min. NRK-52E cells migrating at a speed of at least 20 μm/hr were selected for the experiments involving the interaction between a migrating cell and a stalled/spreading cell. Cells were considered stalled at an intersection if the nucleus remained within 20 μm of the intersection. Symmetry breaking was determined based on morphology symmetry and rates of spreading in opposite directions. Positive responses of stalled cells to contact were recorded if a cell's nucleus migrated >20 μm away from an approaching cell or toward a retreating by 6 hrs after contact. Observations at X or T intersections were limited to interactions of single cells.
Statistical analysis. Tail following behavior observed on Y junctions was assessed based on the probability of a cell to follow its predecessor through the intersection. Under the null condition where cells do not follow their neighbors, cells were assumed to migrate into each branch with equal probability (although they may prefer the open branch due to the greater free space). Statistical significance was determined through one-sample T-tests against 0.5 with p-values of 0.05 as the threshold of significance.
Measurements of contact-dependent responses at X or T intersections were based on the bias of probability of migration in a specific direction after interaction with a neighboring cell. Null condition assumes that cells migrate into any open branch with equal probability. Statistical significance was determined through one-sample binomial tests with p-values of 0.05 as the threshold of significance (8).
Statistical significance of facilitated symmetry breaking was determined by comparing the time of symmetry breaking for cells with or without interacting with a neighboring cell using two-sample T-tests with p-values of 0.05 as the threshold of significance.
Quantification of cell train migration. Phase contrast images were taken every 10 min over 12 hrs with an electron multiplication CCD camera (iXon DV887DCS-BV; Andor Technology, South Windsor, CT) attached to a Nikon Eclipse Ti microscope equipped with a 10x or 40x PlanFluor dry phase contrast objective lens. The nucleus of each cell was used as reference for the analysis of migration. Persistence is given as a ratio of net migration distance divided by the total path length.
Fixation and immunostaining. NRK-52E cells were followed with phase contrast optics over a period of three hours to positively identify migrating or stalled cells. Pairs of cells were observed similarly to confirm if an approaching or retreating cell was interacting with a stalled cell. As soon as cell migration behavior was determined, the cells were fixed immediately in 4% formaldehyde (from 16% stock solution; Thermo Fisher Scientific, Pittsburgh, PA), and stained with rabbit antibodies against non-muscle myosin II-B at a dilution of 1:200 (M7939, Sigma Aldrich, St. Louis, MO), and visualized with goat anti-mouse antibodies at a dilution of 1:1000 (Invitrogen, Carlsbad, CA) (9-10). Actin was stained using rhodamine phalloidin (Molecular Probes, Eugene, OR) for 30 min according to the manufacturer's instructions.
To observe front-rear polarity within collectives, NRK-52E cells were fixed in 4% formaldehyde from 16% stock solution (Thermo Fisher Scientific, Pittsburgh, PA), stained with mouse antibodies against gamma-tubulin at a dilution of 1:1000 (Sigma-Aldrich, St. Louis, MO), and visualized with goat anti mouse antibodies at a dilution of 1:1000 (Invitrogen, Carlsbad, CA). Cell nucleus was stained using Hoechst 33342 at a concentration of 2 ug/mL. Epifluorescence images were acquired with a 40x PlanFluor dry phase contrast objective lens.

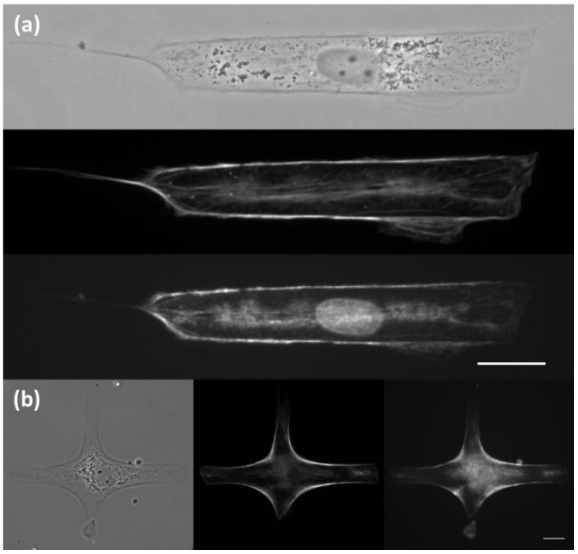

Fig. S1. Actin and NMII-B stains of migrating and stalled NRK-52E cells on micropatterns. Staining of actin with fluorescent phalloidin and immunostaining of NMII-B shows that both actin (a, center) and NMII-B (a, bottom) are predominantly localized to the rear of a cell migrating persistently to the right along a micropatterned line (a, top). Staining also reveals symmetric distribution of both actin (b, center) and NMII-B (b, right) in a cell stalled at an X-junction (b, left). Scale bar, 30 μm.

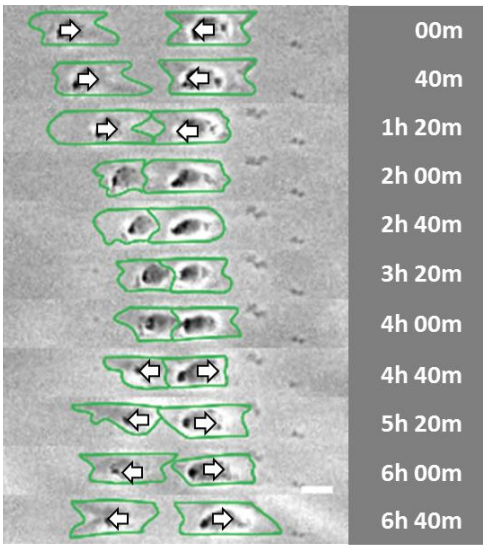

Fig. S2. CIL of NRK-52E cells colliding along a strip. Phase contrast images show two individual cells migrating towards each other on a micropatterned strip, colliding, and reversing the direction. White arrows indicate the direction of migration. Elapsed time shown to the right. Scale bar 30 µm.

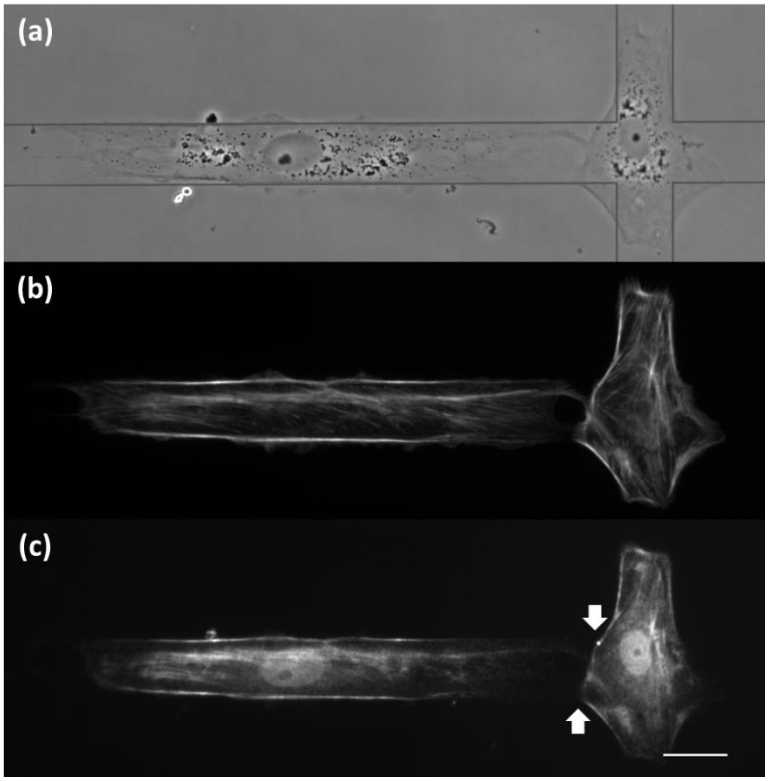

Fig. S3. The distribution of actin and NMII-B in a stalled NRK-52E cell after contacting the head of an approaching cell. Staining of actin with fluorescent phalloidin (b) and NMII-B with antibodies (c) of an approaching cell (left) interacting with a stalled cell at an X-junction (right) shows that the approaching cell is polarized towards the stalled cell and the stalled cell is starting to become polarized away from the head of the approaching cell. White arrows indicate an accumulation of NMII-B in the stalled cell at the site of cell-cell contact. Substrate micropattern is indicated by grey lines. Scale bar, 30 μm.

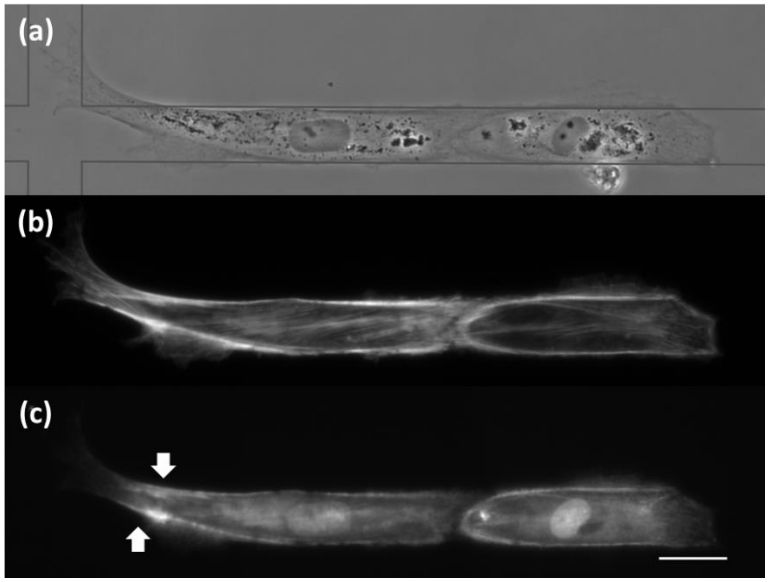

Fig. S4. The distribution of actin and NMII-B in a stalled NRK-52E cell following contact with the tail of a retreating cell. Staining of actin with fluorescent phalloidin (b) and NMII-B with antibodies (c) of a retreating cell (right) interacting with a stalled cell at a X-junction (left) shows that the retreating cell is polarized away from the stalled cell and the stalled cell is polarized towards the tail of the retreating cell. White arrows indicate an accumulation of NMII-B in the stalled cell opposite to the site of cell-cell contact. Substrate micropattern is indicated by grey lines. Scale bar, 30 μm.

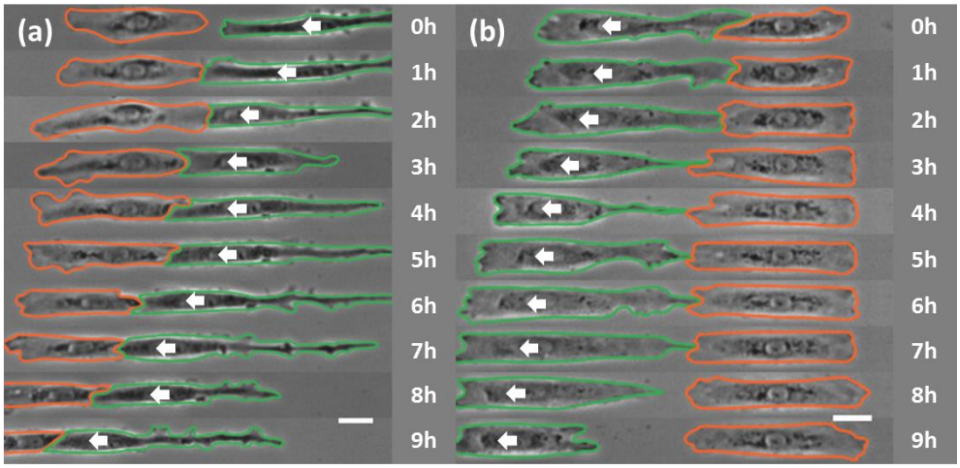

Fig. S5. Inhibition of CFL, but not CIL, during cell-contact mediated symmetry breaking by the Dvl inhibitor 3289-8625. (a) Phase contrast images show a spreading NRK-52E cell from the second round of seeding (red), making contact with and migrating away from the head of an approaching cell (green) in the presence of 10 μM of 3289-8625. (b) Phase contrast images of a spreading cell from the second round of seeding (red) making contact with and failing to follow the tail of a retreating cell (green) in the presence of 10 μM of 3289-8625. White arrows indicate the direction of migration of the cell from the first round of seeding. Elapsed times are shown to the right. Scale bar, 30 μm.

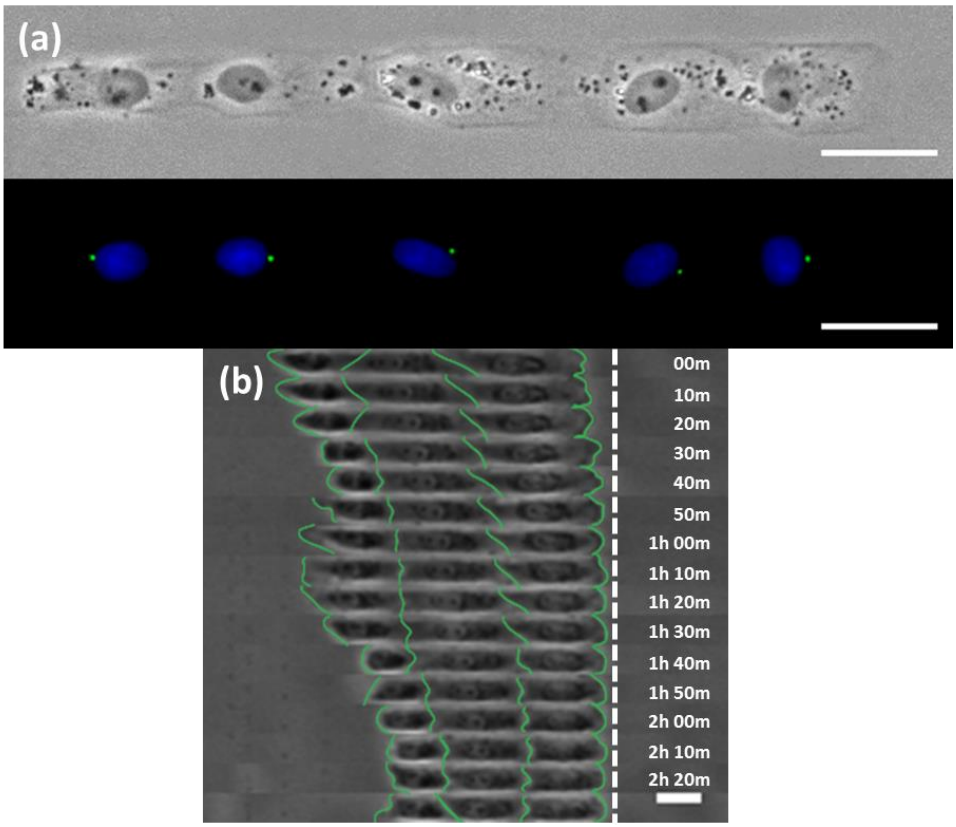

Fig. S6. Active collective migration of NRK-52E cells. Immunofluorescence staining of gamma-tubulin shows that centrosomes (a, green) in a collective train are positioned in front of the nuclei (counter-stained with Hoechst 33258, blue), except for the trailing cell at the left hand side. Stalling of the leader cell at the end of a strip does not immediately halt the forward migration of the rest of cells (b). Dotted line indicates the end of the micropatterned strip and green lines indicate cell borders. Trains are migrating to the right. Elapsed times are shown to the right. Scale bar, 30 μm.

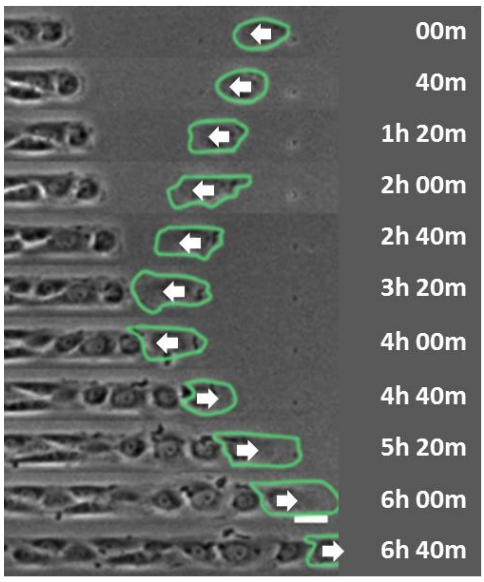

Fig. S7. Incorporation of single cells into a collective following head-on collision. Phase contrast images show the collision of a train of NRK-52E cells (left) with an individual cell (right, green) on a micropatterned strip. Following the collision, the individual cell reversed the direction, while the train continued the migration to turn the individual cell into its new leader. White arrows indicate the direction of migration of the individual cell. Elapsed times are shown to the right. Scale bar, 30 μm.

Table S1. Effects of Dvl inhibition on individual NRK-52E cell migration

	Velocity (μm/min)	Persistence
Control	0.21 ± 0.02 (n=44)	0.70 ± 0.04 (n=30)
NSC 668036	0.19 ± 0.02 (n=16) ^{NS}	0.71 ± 0.05 (n=13) ^{NS}
3289-8625	0.23 ± 0.02 (n=23) ^{NS}	0.72 ± 0.04 (n=23) ^{NS}

Individual NRK-52E cells treated with 50 μM NSC 668036 or 10 μM 3289-8625 migrate with similar velocity and persistence as untreated cells on 30 μm micropatterned lines. Persistence is given as a ratio of net migration distance divided by the total path length. Significance was determined using a two-sample T-test against control. NS indicates not significant at $p \geq 0.05$.

Table S2. Responses of NRK-52E cells to head or tail contact after the inhibition of Dvl with 3289-8625

	Retreating from an approaching neighbor		Following a retreating neighbor	
	Control	3289-8625	Control	3289-8625
X intersection	88.2 ± 3.4% (n=93)	81.5 ± 7.6% (n=27)^{NS}	69.4 ± 5.9% (n=62)	40.0 ± 11.2% (n=20)†
Double seeding	73.1 ± 3.5% (n=160)	77.8 ± 5.3% (n=63)^{NS}	71.2 ± 2.8% (n=267)	30.9 ± 5.2% (n=81)†††

NRK-52E cells treated with 10 μM 3289-8625 maintain the ability to migrate away from the head of approaching neighbors (CIL), but lose their ability to migrate towards the tail of retreating neighbors (CFL) in both experimental settings. Significance was determined using a two-sample T-test against control. † indicates $p<0.05$, ††† indicates $p<0.0005$, NS indicates not significant.

Movie S1. NRK-52E cell at an X intersection moving away from an approaching neighbor. Time lapse video of a stalled NRK-52E cell migrating away from the X intersection after interacting with the head of an approaching cell. The first second of the video displays the X intersection where the time lapse was recorded, shown with fluorescent beads. Frames are taken at 10 min intervals. The total duration is 750 min. Scale bar, 50 μm.

Movie S2. NRK-52E cell at a T intersection moving away from an approaching neighbor. Time lapse video of a stalled NRK-52E cell migrating away from the T intersection after interacting with the head of an approaching cell. The first second of the video displays the T intersection where the time lapse was recorded, shown with fluorescent beads. Frames are taken at 10 min intervals. The total duration is 740 min. Scale bar, 50 μm.

Movie S3. NRK-52E cell at an X intersection moving to follow a departing neighbor. Time lapse video of a stalled NRK-52E cell migrating away from an X intersection to follow the tail of a departing neighbor. The first second of the video displays the X intersection where the time lapse was recorded, shown with fluorescent beads. Frames are taken at 10 min intervals. The total duration is 1620 min. Scale bar, 50 μm.

Movie S4. NRK-52E cell at a T intersection moving to follow a departing neighbor. Time lapse video of a stalled NRK-52E cell migrating away from a T intersection to follow the tail of a departing neighbor. The first second of the video displays the T intersection where the time lapse was recorded, shown with fluorescent beads. Frames are taken at 15 min intervals. The total duration is 825 min. Scale bar, 50 μm.

Movie S5. MDCK cell at an X intersection moving away from an approaching neighbor. Time lapse video of a stalled MDCK cell migrating away from an X intersection after interacting with the head of an approaching cell. The first second of the video displays the X intersection where the time lapse was recorded, shown with fluorescent beads. Frames are taken at 10 min intervals. The total duration is 740 min. Scale bar, 50 μm.

Movie S6. NIH 3T3 cell at an X intersection moving away from an approaching neighbor. Time lapse video of a stalled NIH 3T3 cell migrating away from an X intersection after interacting with the head of an approaching cell. The first second of the video displays the X intersection where the time lapse was recorded, shown with fluorescent beads. Frames are taken at 10 min intervals. The total duration is 600 min. Scale bar, 50 μm.

Movie S7. MDCK cell at an X intersection moving to follow a departing neighbor. Time lapse video of a stalled MDCK cell migrating away from an X intersection to follow the tail of a departing neighbor. The first second of the video displays the X intersection where the time lapse was recorded, shown with fluorescent beads. Frames are taken at 10 min intervals. The total duration is 740 min. Scale bar, 50 μm.

Movie S8. NIH 3T3 cell at an X intersection moving to follow a departing neighbor. Time lapse video of a stalled NIH 3T3 cell migrating away from an X intersection to follow the tail of a departing neighbor. The first second of the video displays the X intersection where the time lapse was recorded, shown with fluorescent beads. Frames are taken at 10 min intervals. The total duration is 550 min. Scale bar, 50 μm.

Movie S9. Dvl inhibition disrupts the ability of an NRK-52E cell at an X intersection to follow a departing neighbor. Time lapse video of a stalled NRK-52E cell failing to migrate away from an X intersection to follow the tail of a departing neighbor. Cells were treated with 50 μM NSC

668036 for 12 hrs prior to observation. The first second of the video displays the X intersection where the time lapse was recorded, shown with fluorescent beads. Frames are taken at 10 min intervals. The total duration is 800 min. Scale bar, 50 μm.

Movie S10. Dvl inhibition disrupts the ability of an NRK-52E cell at a T intersection to follow a departing neighbor. Time lapse video of a stalled NRK-52E cell failing to migrate away from a T intersection to follow the tail of a departing neighbor. Cells were treated with 50 μM NSC 668036 for 12 hrs prior to observation. The first second of the video displays the T intersection where the time lapse was recorded, shown with fluorescent beads. Frames are taken at 10 min intervals. The total duration is 980 min. Scale bar, 50 μm.

Movie S11. 3289-8625 disrupts the ability of an NRK-52E cell at an X intersection to follow a departing neighbor. Time lapse video of a stalled NRK-52E cell failing to migrate away from an X intersection to follow the tail of a departing neighbor. Cells were treated with 10 μM 3289-8625 for 12 hrs prior to observation. The first second of the video displays the X intersection where the time lapse was recorded, shown with fluorescent beads. Frames are taken at 10 min intervals. The total duration is 750 min. Scale bar, 50 μm.

Movie S12. NRK-52E cells in a collective follow the tails of their predecessors through a Y junction. Time lapse video of an NRK-52E cell train entering one of the branches of a Y junction. The first second of the video displays the Y junction where the time lapse was recorded, shown in fluorescent beads. Frames are taken at 10 min intervals. The total duration is 400 min. Scale bar, 50 μm.

Movie S13. Dvl inhibition disrupts the ability of NRK-52E cells to follow the tails of their predecessors through a Y junction. Time lapse video of an NRK-52E cell train entering a Y-junction after treatment with 50 μM NSC 668036 overnight. The first second of the video displays the Y junction where the time lapse was recorded, shown in fluorescent beads. Frames are taken at 10 min intervals. The total duration is 700 min. Scale bar, 50 μm.

References

1. Duc-Nguyen H, Rosenblum EN, Zeigel RF (1966) Persistent infection of a rat kidney cell line with Rauscher murine leukemia virus. Journal of Bacteriology 92(4):1133-1140.
2. de Larco JE, Todaro GJ (1978) Epithelioid and fibroblastic rat kidney cell clones: epidermal growth factor (EGF) receptors and the effect of mouse sarcoma virus transformation. Physiology 94(3):335-342.
3. Chang SS, Guo WH, Kim Y, Wang YL (2013) Guidance of Cell Migration by Substrate Dimension. Biophysical Journal 104(2):313-321.
4. Shan J, Shi DL, Wang J, Zheng J (2005) Identification of a specific inhibitor of the disheveled PDZ domain. Biochemistry 44(47):15495-15503.
5. Grandy D, Shan J, Zhang X, Rao S, Akunuru S, Li H, Zhang Y, Alpatov I, Zhang XA, Lang RA, Shi DL, Zheng, JJ (2009) Discovery and Characterization of a Small Molecule Inhibitor of the PDZ Domain of Dishevelled. Journal of Biological Chemistry 284(24):16256-16263.
6. Zhang J, Guo WH, Rape A, Wang YL (2013) Micropatterning Cell Adhesion on Polyacrylamide Hydrogels. Methods in Molecular Biology 1066:147-156.
7. Tse JR, Engler AJ (2010) Preparation of hydrogel substrates with tunable mechanical properties. Current Protocols in Cell Biology 10:doi: 10.1002/0471143030.
8. Clark MPA, Westerberg BD (2009) How random is the toss of a coin? Canadian Medical Association Journal 181(12):E306-E308.

9. Vicente-Manzanares M, Newell-Litwa K, Bachir AI, Whitmore LA, Horwitz AR (2011) Myosin IIA/IIB restrict adhesive and protrusive signaling to generate front-back polarity in migrating cells. Journal of Cell Biology 193(2):381-396.
10. Vicente-Manzanares M, Koach MA, Whitmore L, Lamers ML, Horwitz AF (2008) Segregation and activation of myosin IIB creates a rear in migrating cells. Journal of Cell Biology 183(3):543.